Enforced Long-Range Order in 1D Wires by Coupling to Higher Dimensions

Zamin Mamiyev,[1,2,3,*] Christa Fink,[4] Kris Holtgrewe,[4] Herbert Pfnür,[1,2,†] and Simone Sanna[4,‡]
[1]Institut für Festkörperphysik, Leibniz Universität Hannover, Appelstraße 2, 30167 Hannover, Germany
[2]Laboratorium für Nano- und Quantenengineering (LNQE), Leibniz Universität Hannover, Schneiderberg 39, 30167 Hannover, Germany
[3]Institut für Physik, Technische Universität Chemnitz, Reichenhainer Straße 70, 09126 Chemnitz, Germany
[4]Institut für Theoretische Physik and Center for Materials Research (LaMa), Justus-Liebig-Universität Gießen, Heinrich-Buff-Ring 16, 35392 Gießen, Germany

(Received 2 October 2020; accepted 23 January 2021; published 10 March 2021)

One-dimensional wires are known to be inherently unstable at finite temperature. Here, we show that long-range order of atomic Au double chains adsorbed on a Si(553) surface is not only stabilized by interaction with the substrate, but spontaneous self-healing of structural defects is actually enforced by the adsorption of atomic species such as Au or H. This is true even for random adsorbate distribution. Combining atomistic models within density functional theory with low energy electron diffraction and high-resolution electron energy loss spectroscopy, we demonstrate that this apparently counterintuitive behavior is mainly caused by adsorption-induced band filling of modified surface bands, i.e., by the strong electronic correlation throughout the whole terrace. Although adsorption preferably occurs at the step edge, it enhances the dimerization and the stiffness of the Au dimers. Thus, the intertwinement of quasi-1D properties with delocalized 2D effects enforces the atomic wire order.

DOI: 10.1103/PhysRevLett.126.106101

The reduction of size and dimensionality of metallic objects gives rise to peculiar physical properties such as quantization of conductance, spin-charge separation, charge and spin density waves, and Luttinger liquid behavior [1–5], which are subject of fundamental studies on low-dimensional physics. Unfortunately, free-standing metallic wires cannot be realized due to their inherent instability [5]. This problem can be partially circumvented by the formation of self-assembled, metallic atomic chains on stepped semiconductor surfaces such as Ge and Si, which are regarded as the low-end limit for long-range ordered nanostructures [6–15]. Several realizations of such wire systems have been reported [11,16–21]. While structural embedding is a prerequisite for the realization of 1D wires, the coupling to higher dimensions implies an intricate balance between preservation and destruction of typical 1D instabilities [22]. On the other hand, the coupling to higher dimensions can be exploited to tune wire properties such as morphology and conductivity. Here, we demonstrate a quite unique and unexpected example thereof: the enhanced and even enforced order of atomic chains by *random* adsorption of atoms, as a new mechanism of crossover between 1D and 2D properties. This behavior is in striking contrast to previously investigated adsorbates, which adsorb at random for low concentrations and thus introduce disorder. While an increased order might be expected if the adsorbates build patterns with the same periodicity of existing structures on the surface, it appears counterintuitive as a consequence of randomly distributed adatoms.

Among the metallic wires grown on regularly stepped surfaces, the Si(553)-Au is one of the most studied systems, due to its relatively high stability, and because of a long-standing debate concerning its exact atomic structure [11,18,19,23–27]. It is commonly accepted that the system features a Si honeycomb and a Au double chain on each terrace. The Au chain is dimerized (even in the absence of adsorbates), which leads to a $\times 2$ periodicity along the terraces. Several attempts to tune the conductivity of this system by deposition of oxygen [28,29] or hydrogen [30–32] are available in the literature. They demonstrate an intricate scenario with adsorbate specific modifications of the electronic structure. Generally, different adsorption sites of similar energy are available on the surface, leading to a random adsorbate distribution and a complex modification of the electronic structure.

In this Letter, we demonstrate the improvement of the dimerized Au chain order simply by adsorption of small amounts of surplus Au, or of atomic H at room temperature. Since these adsorbates, as shown in the following, adsorb at random sites, this effect does not depend on the formation of ordered adsorbate arrays. Density functional theory (DFT) calculations show that the observed behavior stems from the coupling of the 1D atomic chains to higher dimensions. The electronic structure is modified by the effective electron donation from the adsorbates. The latter affects nonlocally the atomic arrangement of the whole terrace, demonstrating the extreme electronic correlation in this quasi-1D system. The rearranged structure is by far less

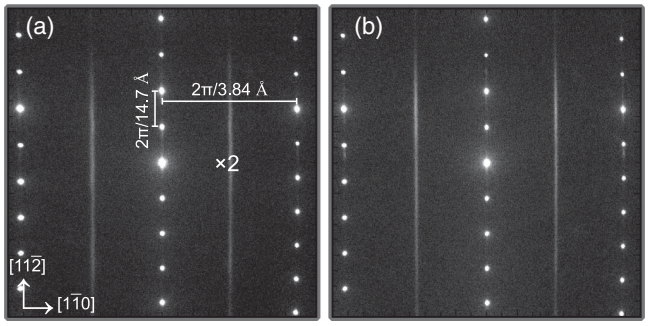

FIG. 1. (a) SPA-LEED patterns of the Si(553) surface with 0.48 ML of Au. (b) After deposition of 0.03 ML surplus Au. All images were recorded at RT with primary energy of 138 eV.

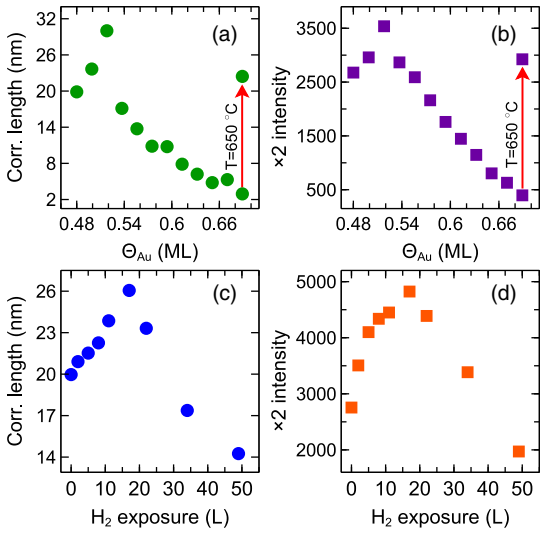

FIG. 2. Correlation length along Au chains (a),(c) and change of ×2 intensity (b),(d) as a function of the surplus Au coverage (a),(b) and of atomic H adsorption (c),(d). Datasets were deduced from line scans in the [1$\bar{1}$0] direction after fitting with convoluted Lorentzian and Gaussian functions. Only about 1% of the given exposure was atomic hydrogen.

prone to structural defects, which results in a further increase of the system order.

This phenomenon is demonstrated by low energy electron diffraction (LEED). A LEED image for Si(553)-Au after adsorption of 0.48 ML of Au, the optimal concentration for double-chain formation, prepared as described in the Supplemental Material [33], is shown in Fig. 1(a). According to Ref. [22], the streaks between first order spots in [1$\bar{1}$0] direction are caused by an ordered dimerization within the double Au chains on each terrace. The small wiggly modulation of these streaks indicates some residual correlation of the dimerization between adjacent terraces. The LEED pattern after deposition of a surplus of 0.03 ML of Au at RT is shown in Fig. 1(b). While the LEED pattern at first glance seems to be unchanged, the integrated intensity of the ×2 streaks is clearly increased. At the same time, the streaks get sharper and appear as unmodulated straight lines, indicating an increased amplitude of dimerization and the complete loss of correlation between adjacent terraces. Interestingly, a very similar behavior can be observed by adsorption of atomic H [30], as we show below.

In order to get more insight into the structural modifications of this surface under H and Au deposition, we determined an average structural correlation length for the ×2 periodicity from the inverse half width (FWHM) of the Lorentzian contribution of the spot profiles. For this purpose, the line profiles along the [1$\bar{1}$0] direction were fitted by a convolution of Lorentzian and Gaussian functions. The results from this fit routine are shown in Fig. 2. Up to a Au surplus concentration of 0.04 ML, the ×2 correlation length increases by a factor of 1.6 to a maximum value of 32 nm, whereas further adsorption of Au leads to a sharp reduction of this quantity. Performing a similar measurement with atomic H, a similar behavior of half widths and intensity of the ×2 streaks in LEED is observed, as shown in Figs. 2(c) and 2(d). The measurements reveal a correlation enhancement along the double chains and the concomitant increase of the integrated intensity, coupled with a loss of correlation of the ×2 streaks between different terraces. Please note that only a small fraction of the dose of molecular H_2 is dissociated on the hot filament during exposure, so that the amount of atomic H at the maximum corresponds to about 15% ML, according to the estimate derived in Ref. [34].

After annealing the samples with total Au coverage of 0.52 ML (and higher up to 0.68 ML) at 650 °C, the intensities and the half widths of the ×2 streaks are restored. In addition, a $\sqrt{3} \times \sqrt{3}$ structure appears (shown in Supplemental Material [33]). This indicates a phase separation into atomic wires and small islands with $\sqrt{3}$ structure with a local concentration of 1 ML [35]. This mixed phase is not considered here in more detail.

In order to understand the origin of the enhanced order upon Au and H adsorption, we performed atomistic calculations within the DFT (computational details in the Supplemental Material [33]). While the impact of atomic H has been modeled recently [30,31] providing evidence for random adsorption, we concentrate here on the seemingly very dissimilar system of adsorbed surplus Au atoms. The experimentally observed similarity concerning the improved order in the double Au chains suggests common mechanisms to be identified here. Irrespective of the starting structural model among those proposed in the literature (spin chains [11,25] or rehybridized [26,27] models), the surface features terraces with step edge atoms at roughly the same height after Au adsorption, similar to the original wire model [19]. Potential energy surface (PES) calculations as performed, e.g., in Ref. [46] reveal a strong preference for the Au adsorption at the Si step edge, which is similar to the behavior of H [30,31]. A structural optimization, starting

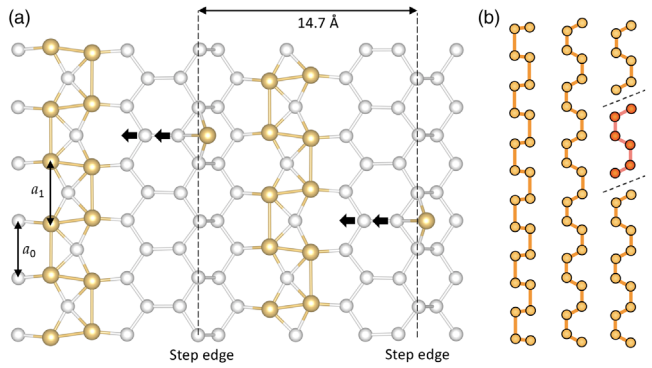

FIG. 3. (a) Optimized Si(553)-Au surface with Au adsorbed at the Si step edge. The surplus coverage corresponds to 1 Au per (5×6) unit cell, or 0.03 ML. Si is white, Au is yellow, a_0 is the Si(111) lattice constant. (b) Schematic representation of the Au chains, before and after Au adsorption, or with an antiphase segment between two idealized stacking faults.

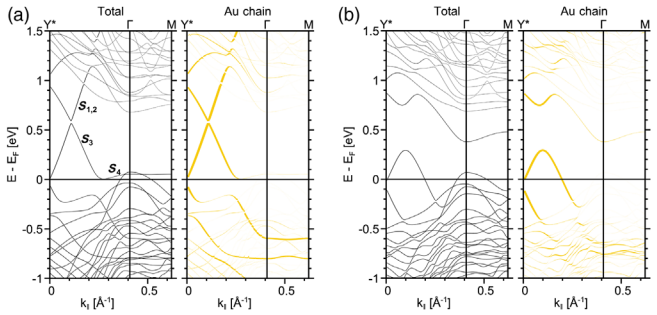

FIG. 4. Band structures calculated within DFT-PBE for (a) the clean and (b) Au-adsorbed Si(553)-Au surface as modeled with a (5×2) surface unit cell. The left panel shows in each case the total band structure, the right panel the Au contribution.

from the minima of the PES, leads to the surface morphology shown in Fig. 3(a). In the optimized position, the Au atom binds with high adsorption energy of −3.9 eV between two Si step edge atoms at a distance of 2.40 Å from them. This is different from H, which adsorbs on top of a step edge atom with a bond length of 1.50 Å. Although a surplus coverage of exactly 0.1 ML Au might result in the formation of a regular Au array at the Si step edge, ordered adsorption is not expected due to energetics and kinetic effects further quantified in the Supplemental Material [33].

Although the adsorption of both Au and H occurs at the step edge, the most relevant adsorption-induced structural modifications are nonlocal and occur at the double Au chain. The Au adsorption at the step edge enhances the chain dimerization $d_{\mathrm{Au}} = (a_1 - a_0)/a_0$ from the value $d_{\mathrm{Au}} = 0.006$ of the clean surface to $d_{\mathrm{Au}} = 0.126$ for 0.1 ML surplus Au. Furthermore, the dimerization is now slightly asymmetric (see Fig. 3).

The enhanced dimerization results from two contributions. The first contribution, as we suggested for the H adsorption [30], is the electron transfer occurring from the donorlike adsorbates to the Au-related electronic bands [22,30]. The resulting modifications in the band structure are shown in Fig. 4, where the total band structure as well as the contribution of the Au atoms are represented. The Au adatom hybridizes with the Si step edge and provides electronic charge, which is mainly transferred to the neighboring Si atoms. Correspondingly, the step edge-related band of the clean surface just above the Fermi energy (labeled S_4) is filled and shifted downward. At the same time, the charge transfer to the Au chain opens a band gap between the two Au-related bands ($S_{1,2}$, S_3) at about $k_{\parallel} = 0.1$ Å^{-1}. While this effect is known from the H adsorption, its magnitude is by far more pronounced in the case of Au adsorption.

In order to prove that this first effect is of a pure electronic nature, irrespective of which mechanism provides the excess electrons, we modified step by step the band occupation and measured the dimerization of the Au chain, as shown in Fig. 5. The band occupation is increased by pure electron injection [Fig. 5(a)] or by gradually allowing the $sp^2 + p$ hybridization [26] with a stepwise step edge modification, quantified by the reaction coordinate q [Fig. 5(b)]. The error bars represent the largest local deviation from the averaged d_{Au} and thus measure the chain asymmetry.

The dimerization is a monotonic function of electron doping and reaction coordinate, and the chain asymmetry grows with the dimerization. Upon pure electron doping, the dimerization starts to grow abruptly only when the surplus electrons fill the Au-related bands, while the

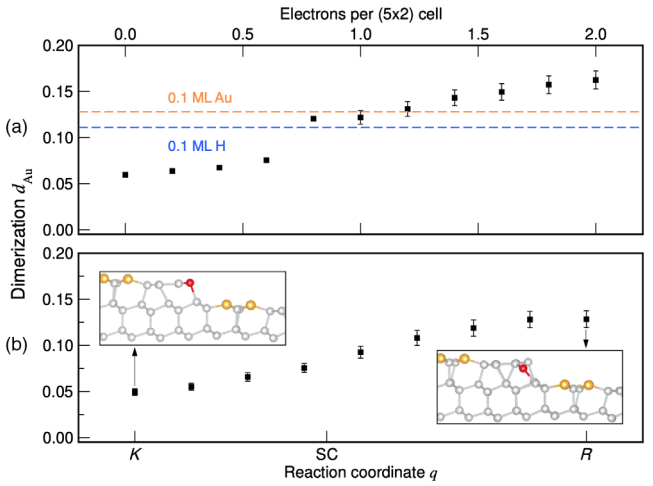

FIG. 5. Calculated dimerization d_{Au} of the Au chain of the clean Si(553)-Au surface upon electron doping (a) or as a function of the reaction coordinate q (b). The latter is roughly given by the vertical position of each third Si step edge atom, and joins the Krawiec (K) and the rehybridized (R) models through the spin-chain (SC) model. The dimerization corresponding to 0.1 ML surplus of Au or H is given by horizontal lines.

rehybridization has a more gradual effect. The dimerization upon adsorption of 1 Au per (5×2) unit cell is slightly larger than the dimerization resulting from an electron doping of one electron per (5×2) unit cell. However, the monovalent Au adatom will hardly provide more than one electron to the substrate.

Indeed, the dimerization enhancement cannot be only explained by electronic transfer. The Au adsorption induces a structural modification of the honeycomb chain next to the adsorption site. The two Si atoms, marked by arrows in Fig. 3(a), are shifted downward and toward the Au chain by about 0.21 Å (right atom) and 0.14 Å (left atom), respectively. This additional structural effect is not observed upon H adsorption, due to the much lower local lattice relaxation of the step edge. This could explain the differences between the dimerization enhancements upon adsorption of 0.1 ML of H (from $d_{\mathrm{Au}} = 0.006$ to $d_{\mathrm{Au}} = 0.111$) and Au (from $d_{\mathrm{Au}} = 0.006$ to $d_{\mathrm{Au}} = 0.126$).

A second contribution stabilizes the strongly dimerized Au chain upon Au adsorption. In real samples, stacking faults occur in the Au dimerized chain, which break the long-short sequence of the Au pairs. Stacking faults lower the structural order by inverting the Au dimerization phase, as schematically represented in Fig. 3(b), and cause the smearing of the diffraction spots in electron scattering experiments.

We have estimated the formation energy of a pinned stacking fault for clean and adsorbed Si(553)-Au surfaces. For this purpose, large supercells of $\times 12$ periodicity with two stacking faults are setup and relaxed. This notwithstanding, the calculations model a high density of stacking faults and only provide a rough estimate of their formation energy. The calculations reveal that the formation energy of a stacking fault rapidly grows with the Au dimerization. While the formation energy of a stacking fault amounts to 0.13 eV for the clean surface, it grows to 0.54 eV for the surface with an Au excess coverage of 0.1 ML. Following simple thermodynamics, the stacking fault concentration is reduced by the Boltzmann factor of the formation energy difference, and results in a drastic decrease of defect concentration at room temperature. This effect can be considered as a self-healing of the Au chain, and further enhances the structural order as indeed observed experimentally.

Finally, we employ electron energy loss spectroscopy to prove the validity of our atomistic simulations. The plasmon dispersion can be employed to predict the unoccupied part of the electronic band structure following the procedure described in Ref. [47] and recently applied, e.g., in Refs. [30,34,48]. In particular, the upper boundary of the single particle excitations (ω_+) can be determined from the measured plasmon dispersion and from lower boundary of the electron-hole continuum (ω_-) as extrapolated from the occupied part of the calculated band structure. Electron energy loss spectra from the well annealed and freshly prepared surface with various surplus Au concentrations at room temperature have been measured (see Supplemental Material [33]). The upper boundary of the single particle excitations as extrapolated from the plasmon dispersion of the adsorbed system is shown, together with the calculated band structures of the corresponding system, in Fig. 6. The nearly quantitative agreement of the dispersion of ω_+ with the calculated band structure gives clear evidence for the Au-induced widening of the band gap at about $k_{\parallel} = 0.1$ Å^{-1} predicted by the atomistic calculations. In turn, it validates the corresponding DFT structural model.

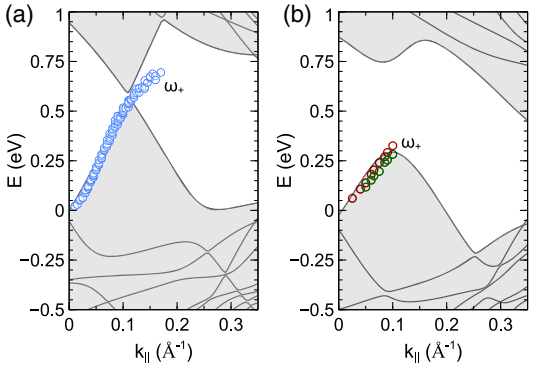

FIG. 6. Calculated electronic band structures for the clean (a) and Au-adsorbed (b) Si(553)-Au surface. The upper boundary of single particle excitations, derived from the plasmon dispersion measured with a Au surplus of 0.00 ML, 0.05 ML, and 0.1 ML is marked by blue, red, and green circles, respectively.

Stabilization of phases or structures by surplus atoms is not limited to the Si(553)-Au surface, but also observed, e.g., for the related Si(111)-(5×2)-Au surface [49,50], which is electronically stabilized by adatoms [51,52]. Au deposition at the Si(111)-Au surface increases the critical temperature to disorder [53] by stabilizing the domain walls between the three equivalent (5×2) domains [48], which are the 2D counterpart to the 1D stacking faults of the Si(553)-Au. Instead, Au adsorption at the Si(775)-Au surface has a similar effect as in the case of the Si(553)-Au system, as revealed by our DFT calculations, although the impact on the Au chain is somewhat less pronounced. This suggests that the mechanism enforcing the structural order is not restricted to the Si(553)-Au system, but can be applied to a broader class of embedded chain systems. However, it crucially depends on the system dimensionality.

In conclusion, we have demonstrated a unique and unexpected tuning of metallic nanowires by adsorption of atoms. Although the atoms adsorb at random, the order of the atomic chains is enforced by the crossover between 1D and 2D properties. Specifically, the hybridization of the Si surface states with the adsorbed species leads to the formation of strongly dimerized double Au chains. The adsorbate-substrate interaction allows for the long-range ordering of the Au chains at the expense of the loss of a

large part of their 1D character. Direct evidence for the resulting 2D character of the whole system is provided by a modified band filling in the Au-adsorbed structure, as a result of a nonlocal adsorbate-to-substrate electronic charge transfer. Correspondingly, the energy of the plasmons in these more than half filled bands is found to decrease. While adsorption as a local process induces adsorbate-specific local relaxations, charge donation (realized by random adsorption of atomic H or Au) is delocalized and influences terraces as a whole. As a consequence, although the chain atoms are not in direct contact with the adsorbed species, the dimerization of the Au chains is enhanced, which strongly increases the energetic cost of defect formation in the chains. This results in a spontaneous self-healing of defects such as stacking faults within the chains, so that long-range order can be improved even by random adsorption. Thus, we demonstrated the intriguing interplay of local and nonlocal electronic properties in a quasi-1D system that leads to improved long-range structural ordering, strong electronic correlation, self-healing of defects, and to dimensional crossover from 1D to 2D.

We gratefully acknowledge financial support from the Deutsche Forschungsgemeinschaft (research unit FOR1700, Projects No. SA 1948/1-2 and No. TE 386/10-2) and Niedersächsisches Ministerium für Wissenschaft und Kultur through the graduate school "contacts in nanosystems." Computational resources are provided by the HPC Core Facility and the HRZ of the Justus-Liebig-Universität Gießen, the TU Darmstadt and the Höchstleistungrechenzentrum Stuttgart (HLRS).

*zamin.mamiyev@physik.tu-chemnitz.de
†pfnuer@fkp.uni-hannover.de
‡simone.sanna@theo.physik.uni-giessen.de

[1] S. Kagoshima, H. Nagasawa, and T. Sambongi, in *One-Dimensional Conductors*, Springer Series in Solid-State Sciences Vol. 72 (Springer Berlin Heidelberg, Berlin, Heidelberg, 1988), pp. 126–135.
[2] G. Grüner, Rev. Mod. Phys. **60**, 1129 (1988).
[3] J. M. Luttinger, J. Math. Phys. (N.Y.) **4**, 1154 (1963).
[4] K. Schönhammer, Luttinger liquids: Basic concepts, in *Strong Interactions in Low Dimensions*, Physics and Chemistry of Materials with Low-Dimensional Structures Vol. 25, edited by L. D. D. Baeriswyl (Springer Netherlands, Dordrecht, 2004), Chap. 4, pp. 93–136.
[5] T. Giamarchi, *Quantum Physics in One Dimension* (Clarendon Press, Oxford, 2007).
[6] A. van Houselt, M. Fischer, B. Poelsema, and H. J. W. Zandvliet, Phys. Rev. B **78**, 233410 (2008).
[7] O. Gurlu, O. A. O. Adam, H. J. W. Zandvliet, and B. Poelsema, Appl. Phys. Lett. **83**, 4610 (2003).
[8] C. Zeng, P. Kent, T.-H. Kim, A.-P. Li, and H. H. Weitering, Nat. Mater. **7**, 539 (2008).
[9] P. C. Snijders and H. H. Weitering, Rev. Mod. Phys. **82**, 307 (2010).
[10] H. Weitering, Nat. Phys. **7**, 744 (2011).
[11] S. C. Erwin and F. J. Himpsel, Nat. Commun. **1**, 58 (2010).
[12] J. Aulbach, J. Schäfer, S. C. Erwin, S. Meyer, C. Loho, J. Settelein, and R. Claessen, Phys. Rev. Lett. **111**, 137203 (2013).
[13] C. Brand, H. Pfnür, G. Landolt, S. Muff, J. H. Dil, T. Das, and C. Tegenkamp, Nat. Commun. **6**, 8118 (2015).
[14] K. Holtgrewe, S. Appelfeller, M. Franz, M. Dähne, and S. Sanna, Phys. Rev. B **99**, 214104 (2019).
[15] T. Lichtenstein, Z. Mamiyev, E. Jeckelmann, C. Tegenkamp, and H. Pfnür, J. Phys. Condens. Matter **31**, 175001 (2018).
[16] J. N. Crain, J. L. McChesney, F. Zheng, M. C. Gallagher, P. C. Snijders, M. Bissen, C. Gundelach, S. C. Erwin, and F. J. Himpsel, Phys. Rev. B **69**, 125401 (2004).
[17] I. Barke, F. Zheng, T. K. Rügheimer, and F. J. Himpsel, Phys. Rev. Lett. **97**, 226405 (2006).
[18] J. Aulbach, S. C. Erwin, R. Claessen, and J. Schäfer, Nano Lett. **16**, 2698 (2016).
[19] M. Krawiec, Phys. Rev. B **81**, 115436 (2010).
[20] I. Miccoli, F. Edler, H. Pfnür, S. Appelfeller, M. Dähne, K. Holtgrewe, S. Sanna, W. G. Schmidt, and C. Tegenkamp, Phys. Rev. B **93**, 125412 (2016).
[21] C. Braun, C. Hogan, S. Chandola, N. Esser, S. Sanna, and W. G. Schmidt, Phys. Rev. Mater. **1**, 055002 (2017).
[22] S. Sanna, T. Lichtenstein, Z. Mamiyev, C. Tegenkamp, and H. Pfnür, J. Phys. Chem. C **122**, 25580 (2018).
[23] S. Polei, P. C. Snijders, S. C. Erwin, F. J. Himpsel, K.-H. Meiwes-Broer, and I. Barke, Phys. Rev. Lett. **111**, 156801 (2013).
[24] S. Polei, P. C. Snijders, K.-H. Meiwes-Broer, and I. Barke, Phys. Rev. B **89**, 205420 (2014).
[25] B. Hafke, T. Frigge, T. Witte, B. Krenzer, J. Aulbach, J. Schäfer, R. Claessen, S. C. Erwin, and M. Horn-von Hoegen, Phys. Rev. B **94**, 161403(R) (2016).
[26] C. Braun, U. Gerstmann, and W. G. Schmidt, Phys. Rev. B **98**, 121402(R) (2018).
[27] C. Braun, S. Neufeld, U. Gerstmann, S. Sanna, J. Plaickner, E. Speiser, N. Esser, and W. G. Schmidt, Phys. Rev. Lett. **124**, 146802 (2020).
[28] F. Edler, I. Miccoli, J. P. Stöckmann, H. Pfnür, C. Braun, S. Neufeld, S. Sanna, W. G. Schmidt, and C. Tegenkamp, Phys. Rev. B **95**, 125409 (2017).
[29] Z. Mamiyev, M. Tzschoppe, C. Huck, A. Pucci, and H. Pfnür, J. Phys. Chem. C **123**, 9400 (2019).
[30] Z. Mamiyev, S. Sanna, T. Lichtenstein, C. Tegenkamp, and H. Pfnür, Phys. Rev. B **98**, 245414 (2018).
[31] C. Hogan, E. Speiser, S. Chandola, S. Suchkova, J. Aulbach, J. Schäfer, S. Meyer, R. Claessen, and N. Esser, Phys. Rev. Lett. **120**, 166801 (2018).
[32] M. Tzschoppe, C. Huck, F. Hötzel, B. Günther, Z. Mamiyev, A. Butkevich, C. Ulrich, L. Gade, and A. Pucci, J. Phys. Condens. Matter **31**, 195001 (2019).
[33] See Supplemental Material at http://link.aps.org/supplemental/10.1103/PhysRevLett.126.106101, which includes Refs. [11,19,26,27,30,31,34–45], for more details.
[34] Z. Mamiyev, T. Lichtenstein, C. Tegenkamp, C. Braun, W. G. Schmidt, S. Sanna, and H. Pfnür, Phys. Rev. Mater. **2**, 066002 (2018).

[35] T. Nagao, S. Hasegawa, K. Tsuchie, S. Ino, C. Voges, G. Klos, H. Pfnür, and M. Henzler, Phys. Rev. B **57**, 10100 (1998).
[36] J. P. Perdew, A. Ruzsinszky, G. I. Csonka, O. A. Vydrov, G. E. Scuseria, L. A. Constantin, X. Zhou, and K. Burke, Phys. Rev. Lett. **100**, 136406 (2008).
[37] G. Kresse and J. Furthmüller, Comput. Mater. Sci. **6**, 15 (1996).
[38] G. Kresse and J. Furthmüller, Phys. Rev. B **54**, 11169 (1996).
[39] G. Kresse and D. Joubert, Phys. Rev. B **59**, 1758 (1999).
[40] P. E. Blöchl, Phys. Rev. B **50**, 17953 (1994).
[41] H. J. Monkhorst and J. D. Pack, Phys. Rev. B **13**, 5188 (1976).
[42] H. Claus, A. Büssenschütt, and M. Henzler, Rev. Sci. Instrum. **63**, 2195 (1992).
[43] F. Hötzel, N. Galden, S. Baur, and A. Pucci, J. Phys. Chem. C **121**, 8120 (2017).
[44] G. Sauerbrey, Z. Phys. **155**, 206 (1959).
[45] B. Halbig, M. Liebhaber, U. Bass, J. Geurts, E. Speiser, J. Räthel, S. Chandola, N. Esser, M. Krenz, S. Neufeld, W. G. Schmidt, and S. Sanna, Phys. Rev. B **97**, 035412 (2018).
[46] Z. Mamiyev, S. Sanna, F. Ziese, C. Dues, C. Tegenkamp, and H. Pfnür, J. Phys. Chem. C **124**, 958 (2020).
[47] T. Lichtenstein, Z. Mamiyev, C. Braun, S. Sanna, W. G. Schmidt, C. Tegenkamp, and H. Pfnür, Phys. Rev. B **97**, 165421 (2018).
[48] Z. Mamiyev and H. Pfnür, Phys. Rev. B **102**, 075438 (2020).
[49] S. C. Erwin, Phys. Rev. Lett. **91**, 206101 (2003).
[50] S. C. Erwin, I. Barke, and F. J. Himpsel, Phys. Rev. B **80**, 155409 (2009).
[51] A. Stępniak, P. Nita, M. Krawiec, and M. Jałochowski, Phys. Rev. B **80**, 125430 (2009).
[52] A. Stępniak, M. Krawiec, G. Zawadzki, and M. Jałochowski, J. Phys. Condens. Matter **24**, 095002 (2012).
[53] J. Kautz, M. W. Copel, M. S. Gordon, R. M. Tromp, and S. J. van der Molen, Phys. Rev. B **89**, 035416 (2014).